

Mini Review

Open Access

# From Silver(I) Exposure to Bacterial Defense: Focus on Sil and Cus Systems

Alexandre Bianchi<sup>1</sup>, and Katharina M. Fromm<sup>1\*</sup>

<sup>1</sup>Univ. Fribourg, Department of Chemistry and National Center of Competence in Research Bio-inspired Materials, Chemin du Musée 9, CH-1700 Fribourg, Switzerland.

## Article Info

### Article Notes

Received: March 11, 2026

Accepted: April 13, 2026

### \*Correspondence:

\*Katharina M. Fromm, Univ. Fribourg, Department of Chemistry and National Center of Competence in Research Bio-inspired Materials, Chemin du Musée 9, CH-1700 Fribourg, Switzerland; Email: [katharina.fromm@unifr.ch](mailto:katharina.fromm@unifr.ch).

© 2026 Fromm KM. This article is distributed under the terms of the Creative Commons Attribution 4.0 International License.

### Keywords:

Silver  
Tolerance  
Gram-negative Bacteria  
Sil and Cus Systems  
Efflux Pump  
Proteins

## Abstract

Silver ions ( $\text{Ag}^+$ ) have been shown to possess antimicrobial properties. However, some Gram-negative bacteria have evolved sophisticated mechanisms to tolerate their toxicity. Among these, the plasmid-encoded Sil system and the chromosomal Cus system are key efflux-based resistance mechanisms. The Sil system is composed of a two-component regulator (SilS and SilR), periplasmic chaperones (SilF, SilG, and SilE), a P-type ATPase (SilP), and a tripartite efflux pump (SilABC) to sense, sequester, and export  $\text{Ag}^+$ . SilE, a small periplasmic protein, plays a pivotal role by binding multiple  $\text{Ag}^+$  through histidine and methionine residues, which undergo a transition from disordered to  $\alpha$ -helical conformations upon  $\text{Ag}^+$  coordination. A comparative analysis with the Cus system reveals that, while CusF and CusABC perform analogous metal-binding and efflux functions, Cus primarily targets  $\text{Cu}^+$  and lacks auxiliary components such as SilP and SilE. Collectively, these two systems demonstrate the adaptive strategies that bacteria have developed to regulate toxic metal ion concentrations.

## Generalities

Silver ions ( $\text{Ag}^+$ ) exhibit a distinctive combination of chemical and biological properties that serve as the foundation for their antimicrobial activity<sup>1</sup>. However, a variety of microorganisms have evolved sophisticated mechanisms to moderate  $\text{Ag}^+$  cytotoxicity effects. Two primary strategies have been identified: the active extrusion of  $\text{Ag}^+$  via specialized efflux pump systems and the enzymatic reduction of  $\text{Ag}^+$  to  $\text{Ag}^0$ , which exhibits significantly reduced reactivity<sup>2-5</sup>.

Despite the heterogeneity of their biochemical mechanisms, these pathways converge on a common objective: regulating silver concentrations<sup>2,4</sup>. This phenomenon highlights two main points. First, it demonstrates the remarkable adaptive capacity of microorganisms. Second, it reveals the inherent challenges associated with the therapeutic application of silver.

Among bacterial defense mechanisms, efflux pumps constitute a central strategy for controlling intracellular metal ion concentrations<sup>6,7</sup>. These systems export metal ions to prevent toxic accumulation while maintaining essential cellular functions<sup>8</sup>. Efflux pumps exhibit structural and functional diversity across bacterial species<sup>6</sup>. In Gram-positive bacteria, such as *Staphylococcus aureus* (*S. aureus*) and *Enterococcus* species, metal ion extrusion is generally mediated by single polypeptide transporters embedded in the cytoplasmic membrane. These transporters operate through ATP hydrolysis or the proton motive force<sup>8</sup>. In contrast, Gram-negative

bacteria, such as *Escherichia coli* (*E. coli*) and *Salmonella enterica*, rely on multiprotein efflux assemblies that cross both the inner and outer membranes, forming a continuous channel for metal ion transport<sup>7,8</sup>.

Among these Gram-negative bacteria, two homologous efflux pumps, the Sil (Figure 1, left side) and Cus (Figure 1, right side) systems, have attracted particular attention due to their shared architecture and partially overlapping roles in Ag<sup>+</sup> tolerance<sup>2,9</sup>. Although the Sil system performs a comparable detoxification through coordinated sensing, sequestration, and export of Ag<sup>+</sup>, the system exhibits distinct structural and regulatory characteristics<sup>2</sup>.

The Sil system (Figure 1, left side), initially characterized on the pMG101 plasmid of *Salmonella enterica serovar typhimurium*, also known as *Salmonella typhimurium* (*S. typhimurium*), was identified during a hospital outbreak in the 1970s involving burn patients treated with silver-based dressings, where certain *Salmonella* strains exhibited unexpected silver tolerance<sup>10,11</sup>. Genetic analysis revealed a complex operon encoding eight principal proteins, and occasionally a ninth, including SilG (previously referred to as ORF105, and which is non-essential within the sil operon), which act cooperatively to sense and expel Ag<sup>+</sup> from the bacteria<sup>9</sup>. The Sil system consists of a two-component regulatory module (SilSR), a P-type ATPase (SilP), three periplasmic metal-binding proteins (SilF, SilG, SilE), and a tripartite efflux pump (SilABC)<sup>9,12</sup>. In 2015, Randall *et al.* investigated the functional contribution of individual Sil protein by generating targeted deletion mutants in *E. coli* J35 (pMG101)<sup>9</sup>. They demonstrated that deletion of the genes encoding the tripartite efflux pump components (SilABC) or the periplasmic protein (SilE) caused a significant decrease in silver tolerance.

Indeed, the MIC for AgNO<sub>3</sub> decreases from >256 mg/L

to 4-8 mg/L<sup>9</sup>. In contrast, deletion of the P-type ATPase (SilP) and both periplasmic chaperones (SilF and SilG) had a markedly weaker effect on silver tolerance<sup>9</sup>.

Conversely, the Cus system (Figure 1, right side), encoded chromosomally in *E. coli*, represents one of the most well-studied metal efflux mechanisms in Gram-negative bacteria<sup>13-15</sup>. Genetic analysis have identified the presence of an operon encoding 6 proteins that act cooperatively to sense, bind, and export Cu<sup>+</sup> and, to a more limited capacity, Ag<sup>+</sup> from the bacteria<sup>16</sup>. The Cus system is composed of a two-component regulator module (CusSR), a periplasmic chaperone (CusF), and a tripartite efflux pump (CusABC)<sup>13,16</sup>.

Despite their comparable structural architecture, the two systems differ in genetic localization, metal selectivity, and regulator complexity<sup>2,9,10,15</sup>. The plasmid-encoded Sil system, is believed to have originated from the chromosomal Cus system, with natural selection favoring mutations that enhanced Ag<sup>+</sup> detoxification through the addition of proteins such as SilP, SilG, and SilE, which enhance Ag<sup>+</sup> binding and extrusion<sup>10,15,17</sup>.

After providing a general overview of their organization, the following sections will compare in more detail the corresponding proteins of the Sil and the Cus system.

### SilSR vs CusSR - The Two-Component Regulator Modules

SilS (497 amino acids, UniProt: Q9ZHD4) and CusS (480 amino acids, UniProt: P77485), which exhibit 55.2 % sequence identity based on BLAST analysis, are two membrane-bound histidine kinases that act as sensory components of the SilSR and CusSR two-component regulator systems, respectively<sup>9,10,12,16,18</sup>. In both proteins, the periplasmic sensing domain detects metal ions (Ag<sup>+</sup>

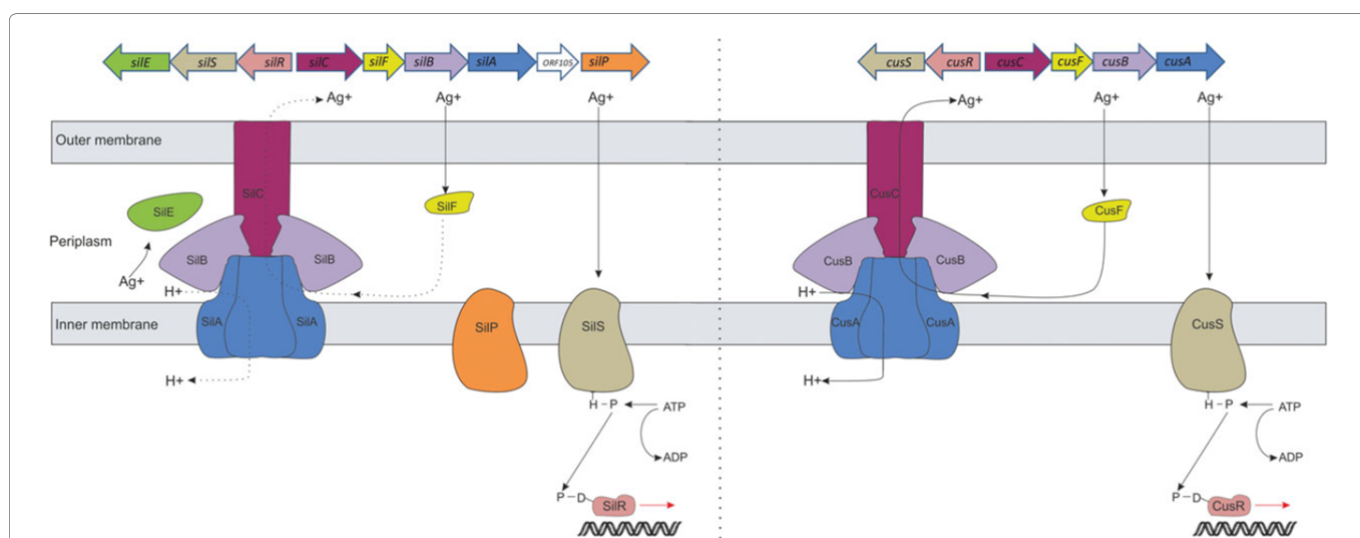


**Figure 1.** Schematic representation of Sil (left side) and Cus (right side) systems, with their associated proteins. Sil: SilS, SilR, SilF, SilABC, SilP, SilG, SilE Cus: CusR, CusF, CusABC (reproduced from ref.<sup>9</sup>, licensed under CC BY 4).

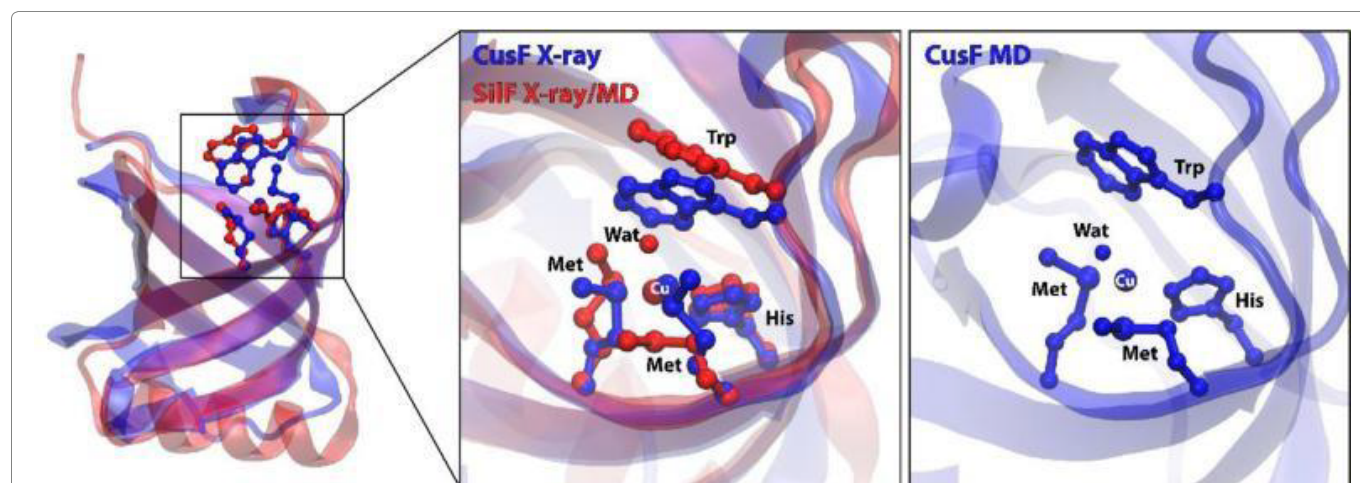


**Figure 2.** Comparison of how  $\text{Cu}^+$  binds in CusF and SilF. X-ray structures reveal that in CusF (blue), the Trp residue is close to the  $\text{Cu}^+$ , whereas in SilF (red), the  $\text{Cu}^+$  is coordinated by a water molecule. Moreover, MD simulations show that the two proteins similarly bind  $\text{Cu}^+$ , with water molecules playing a key role in stabilizing the coordinated  $\text{Cu}^+$  (reproduced from ref.<sup>21</sup>, licensed under CC BY 4.0).

for SilS; principally  $\text{Cu}^+$  for CusS, with  $\text{Ag}^+$  sensed at high concentrations), triggering conformational changes in the cytoplasmic domain that activate ATP hydrolysis to ADP and lead to autophosphorylation of a conserved histidine residue<sup>14,16,19,20</sup>. The phosphoryl group is then transferred to the response regulator SilR or CusR<sup>9</sup>.

SilR (228 amino acids, UniProt: Q9ZHD3) and CusR (227 amino acids, UniProt: P0ACZ8), which exhibit 82.4 % sequence identity based on BLAST analysis, adopt an active conformation upon phosphorylation, which facilitates binding to specific promoter regions within their respective operon<sup>9,12,16,18</sup>. The activation of SilR induces transcription of genes that encode the tripartite efflux pump (SilABC) and its associated proteins (SilF, SilG, and SilP), which mediate  $\text{Ag}^+$  detoxification and export<sup>9,12</sup>. However, the transcription of SilE is controlled by its own promoter and thus occurs independently of the SilR-regulated efflux operon.<sup>2</sup> In contrast, CusR activates the Cus operon, thereby promoting the expression of the tripartite efflux pump (CusABC) and the periplasmic chaperone (CusF)<sup>9</sup>. These proteins mediate the  $\text{Cu}^+$  binding and export and, to a more limited capacity,  $\text{Ag}^+$  detoxification<sup>9</sup>.

### SilF vs CusF - The Periplasmic Chaperones

SilF (117 amino acids, UniProt: A0A707TFN4) and CusF (110 amino acids, UniProt: P77214), which exhibit 47.0 % sequence identity based on BLAST analysis, are two periplasmic chaperones.<sup>9,18</sup> Both proteins adopt a  $\beta$ -barrel structure in their both apo- and holo-forms (Figure 2), creating a metal-binding pocket at the end of the  $\beta$ -barrel structure<sup>21,22</sup>.

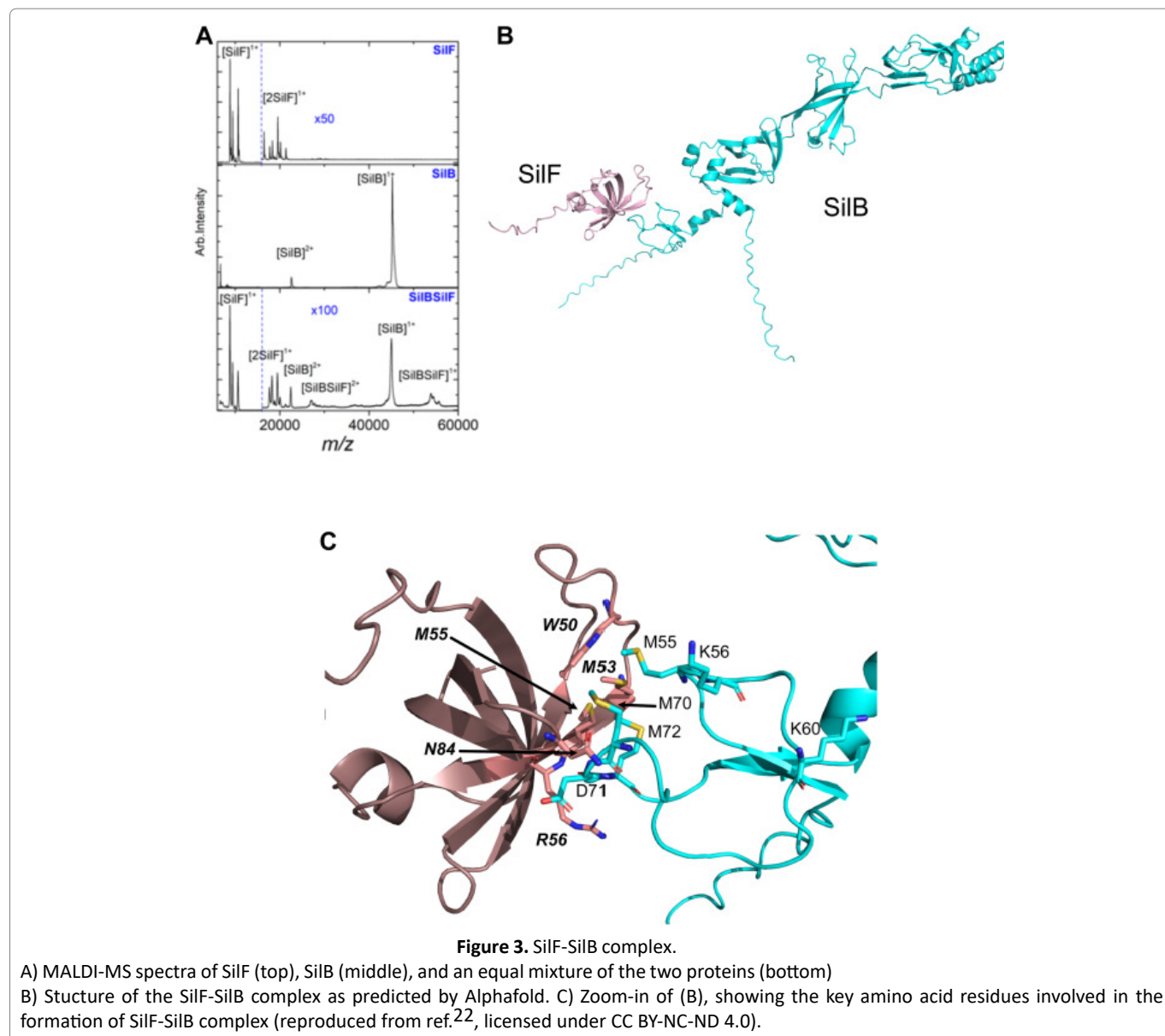
At the periplasmic level, SilF and CusF regulate metal ion trafficking by temporarily sequestering a single metal ion and delivering it to the corresponding tripartite efflux pumps, SilABC or CusABC, respectively. Within the binding pocket,

the metal ion is coordinated by specific amino acid residues, including histidine (His63) and methionine (Met74 and Met76), which together create an appropriate environment for binding a single metal ion, i.e.  $\text{Cu}^+$  and  $\text{Ag}^+$ <sup>21</sup>. Moreover, a conserved tryptophan (Trp71) residue has been shown to stabilize the bound metal ion *via* a cation- $\pi$  interaction, contributing to the distorted trigonal planar geometry of the binding site (Figure 2)<sup>21-23</sup>. The high degree of structural and functional similarity between the two proteins, including the conservation of the key metal-binding amino acid residues, explains their ability to bind both  $\text{Ag}^+$  and  $\text{Cu}^+$ , which possess both a  $d^{10}$  electronic configuration<sup>21</sup>.

More recently, Arrault *et al.* demonstrated that SilF forms a specific protein-protein interface with the periplasmic adaptor protein domain of SilB, even in the absence of  $\text{Ag}^+$  (Figure 3)<sup>22</sup>. This interaction, which is distinct from the metal-binding amino acid residues, is fundamental for efficient  $\text{Ag}^+$  transfer from SilF to SilB. In the presence of SilB, the dissociation constant of  $\text{Ag}^+$  from SilF increases from  $9.5 \pm 3.5 \mu\text{M}$  to  $33.7 \pm 7 \mu\text{M}$ , while the dissociation rate increases approximately by a factor of eight, from  $25.4 \pm 4.5 \text{ s}^{-1}$  to  $198 \pm 27 \text{ s}^{-1}$ . These kinetic changes are consistent with the temporary formation of an intermediate complex: SilF- $\text{Ag}^+$ -SilB. This mechanism ensures directional transfer of  $\text{Ag}^+$  to the SilABC efflux pump by minimizing non-specific interactions in the periplasm<sup>22</sup>.

### SilABC vs CusABC - The Tripartite Efflux Pumps

SilABC (SilA: 1048 amino acids, UniProt: Q9ZHC9; SilB: 430 amino acids, UniProt: Q9ZHD0; SilC: 461 amino acids, UniProt: Q9ZHD2) and CusABC (CusA: 1047 amino acids, UniProt: P38054; CusB: 407 amino acids, UniProt: P77239; CusC: 457 amino acids, UniProt: P77211), which exhibit 87.0 %, 67.4 %, and 71.4 % sequence identity based on BLAST analysis, respectively, are two tripartite Resistance-



Nodulation-Division (RND)-type efflux pumps responsible for the metal ion extrusion<sup>13,18,24,25</sup>. Both systems traverse the inner membrane, the periplasm, and the outer membrane through the assembly of three components: an inner membrane transporter (SilA or CusA), a periplasmic adaptor protein (SilB or CusB), and an outer membrane channel (SilC or CusC). This assembly forms a continuous transmembrane channel that enables efficient metal ion export<sup>13,22,25</sup>.

Both inner membrane components serve as the active transport units of their respective tripartite systems<sup>13,24,25</sup>. Both proteins assemble as trimers and contain large periplasmic domains enriched in conserved methionine residues, which are well suited for coordinating metal ions, such as  $Ag^+$  and  $Cu^+$ <sup>13,24,25</sup>. These transporters use the proton motive force across the inner membrane to actively extract metal ions from the periplasm and drive their extrusion into the extracellular environment.<sup>13,24,25</sup>

Both periplasmic adaptor proteins mediate the connection between the inner membrane transporter and the outer membrane channel. Rather than acting as transporters themselves, these hexameric proteins serve as relay and activation sites<sup>13,22,25</sup>. These proteins interact temporarily with the corresponding periplasmic chaperones SilF or CusF, facilitating the delivery of metal ions within the periplasm.<sup>13,22,25</sup> Metal ion binding has been shown to induce conformational changes in SilB or CusB, thereby promoting stable assembly with SilA or CusA and facilitating metal ion capture<sup>13,22,25</sup>.

Both outer membrane channels form a passive trimeric  $\beta$ -barrel structure in both apo- and holo-forms.<sup>13,26</sup> The interior of these channels is protected from periplasm and coated by electronegative amino acid residues<sup>26</sup>. This architecture ensures that, once extracted by efflux machinery, metal ions are efficiently expelled into

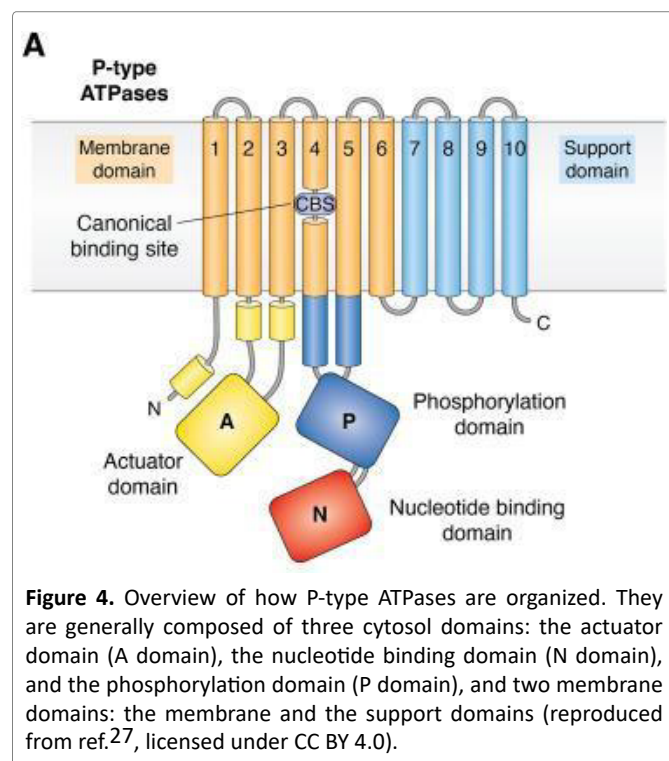


**Figure 4.** Overview of how P-type ATPases are organized. They are generally composed of three cytosol domains: the actuator domain (A domain), the nucleotide binding domain (N domain), and the phosphorylation domain (P domain), and two membrane domains: the membrane and the support domains (reproduced from ref.<sup>27</sup>, licensed under CC BY 4.0).

the extracellular environment, without loss through diffusion<sup>13,25</sup>.

### SilP - The P-Type ATPase

SilP (815 amino acids, UniProt: A0A2S1Q5X5) is an inner membrane P-type efflux ATPase that functions as the cytoplasmic Ag<sup>+</sup> exporter in the Sil system<sup>9,12</sup>. The overall architecture of P-type ATPase (Figure 4) is conserved in SilP, which contains multiple transmembrane helices that form the transmembrane channel for metal ions, along with three domains: the actuator domain (A) domain, the nucleotide-binding domain (N) domain, and the phosphorylation domain (P) domain<sup>27</sup>.

SilP belongs to the P1B subfamily of heavy-metal-transporting ATPases, which use ATP hydrolysis to drive the active transport of metal ions across the inner membrane<sup>27,28</sup>. In contrast to the Cus system, which lacks a P-type efflux ATPase, SilP is functionally analogous to CopA protein, a Cu<sup>+</sup> exporting P1B-type ATPase of *E. coli*<sup>9,28</sup>.

Ag<sup>+</sup> exported by SilP into the periplasm is subsequently captured by periplasmic proteins of the Sil system, including the periplasmic chaperone SilF, and delivered to the SilABC tripartite efflux pump for the final extrusion.

### SilG - The Auxiliary Periplasmic Protein

SilG (146 amino acids, UniProt: A0A4P8WDS2) is a periplasmic protein, initially identified and designated as ORF105 by Gupta *et al.* in 1999, and later renamed SilG by

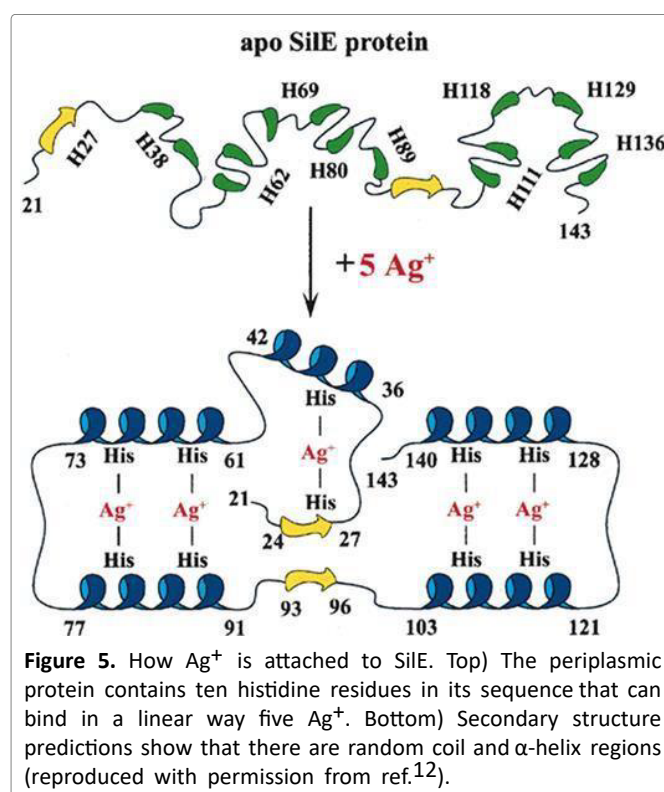


**Figure 5.** How Ag<sup>+</sup> is attached to SilE. Top) The periplasmic protein contains ten histidine residues in its sequence that can bind in a linear way five Ag<sup>+</sup>. Bottom) Secondary structure predictions show that there are random coil and  $\alpha$ -helix regions (reproduced with permission from ref.<sup>12</sup>).

Randall *et al.* in 2015<sup>9,10</sup>. SilG shares approximately 45% sequence similarity to the metal-binding chaperone CopG and contains a repeated Cys-aa-aa-Cys motif<sup>9</sup>. Despite the fact that the precise biological role of SilG remains to be elucidated, its sequence homology and conserved motif suggest a potential role in Ag<sup>+</sup> binding or transfer within the periplasm. It is therefore hypothesized that SilG provides auxiliary support to Ag<sup>+</sup> extrusion.

### SilE - The Periplasmic Protein

SilE (143 amino acids, UniProt: Q9Z4N3) is a unique periplasmic protein whose precise role has long been a mystery and whose secrets have not yet been fully uncovered.

In an initial NMR study conducted on SilE, Silver proposed that the protein could bind up to five Ag<sup>+</sup> via 10 histidine residues (Figure 5)<sup>12</sup>. This finding suggested that SilE plays a pivotal role in sequestering Ag<sup>+</sup>; however, it also assumed that Ag<sup>+</sup> coordination occurred solely through histidine, without considering the potential contribution of other amino acids<sup>12</sup>.

A PhD student, Valentin Chabert from our group, re-examined the amino acid composition of the SilE sequence and found repeat motifs in which methionine was, in most cases, two amino acids away from the histidine moieties. He thus started to investigate tetrapeptide motifs HX2M and MX2H, as found in SilE, in order to determine their binding capacity to Ag<sup>+</sup><sup>29</sup>.

About the same time, Asiani *et al.* identified two different repeating motifs of SilE, MX<sub>2</sub>HX<sub>3</sub>HX<sub>2</sub>MX<sub>2</sub> and HX<sub>2</sub>MX<sub>3</sub>HX<sub>2</sub>MX<sub>2</sub>, which could each contribute to Ag<sup>+</sup> binding<sup>30</sup>. They hypothesized, like Chabert, that the methionine residues might also participate in Ag<sup>+</sup> coordination, but did not have direct experimental evidence at that time<sup>30</sup>. Nevertheless, using spectroscopy analyses (CD, nano-ESI-MS, and ICP-MS), Asiani *et al.* highlighted that SilE undergoes a folding process into an  $\alpha$ -helical structure upon binding to Ag<sup>+</sup>, and that SilE could bind up to eight Ag<sup>+</sup>, with complex formation largely complete after six Ag<sup>+</sup>, indicating the presence of multiple but partially saturable binding sites<sup>30</sup>. The observed variations in reported Ag<sup>+</sup> binding capacities likely reflect both differences in experimental methodologies and the presence of multiple binding, consistent with the heterogeneous binding behavior observed by Asiani *et al.*<sup>30</sup>.

Subsequent crystallographic research from our group provided direct structural evidence that Ag<sup>+</sup> binds to methionine residues (Figure 6), thus validating the dual histidine-methionine coordination mechanism initially hypothesized by Asiani *et al.*<sup>29,30</sup>.

Based on this structural finding and binding affinity studies on tetrapeptides and longer strands excerpt from SilE<sup>12,29-31</sup>, our recent tetrapeptide-based studies have systematically investigated how the nature of intercalating amino acids (X<sub>1,2</sub>) can modulate the Ag<sup>+</sup> binding affinities. Inspired by the repeating motifs found in SilE, tetrapeptides of the types HX<sub>1</sub>X<sub>2</sub>H, MX<sub>1</sub>X<sub>2</sub>M, HX<sub>1</sub>X<sub>2</sub>M, and MX<sub>1</sub>X<sub>2</sub>H were synthesized with various residues X<sub>1</sub> and X<sub>2</sub> (*e.g.* Arg, Lys, Gln, Ala, Pro) to represent the diversity of side chain properties at pH 7.4<sup>32</sup>. It was evident that a clear trend emerged from the peptide library in relation to Ag<sup>+</sup> binding affinity, expressed as log(*K*<sub>ass</sub>)<sup>32</sup>.

It results that peptides containing two histidine (HX<sub>1</sub>X<sub>2</sub>H) exhibited the strongest Ag<sup>+</sup> affinity (*e.g.* 6.0 for HQQH), while peptides with two methionine (MX<sub>1</sub>X<sub>2</sub>M) showed significantly lower affinity (*e.g.* 4.8 for MKKM). This suggests that the sequences with histidine at both coordinating positions favor stronger Ag<sup>+</sup> interactions. It was also noticed that positively charged side chains in the X<sub>1,2</sub> positions tended to reduce affinity in comparison to uncharged residues. Furthermore, the peptide's side chain length and flexibility demonstrated an effect on coordination yet did not result in its complete abolition<sup>32</sup>.

Later, our group also collaborated on a computational study investigating the interactions between Ag<sup>+</sup> and histidine- and methionine-rich motifs in proteins involved in silver tolerance<sup>29,33</sup>. This was achieved by conducting a computational study, which employed all-atom simulations and calibrated CHARMM36m parameters. The study showed that standard force-field parameters underestimate

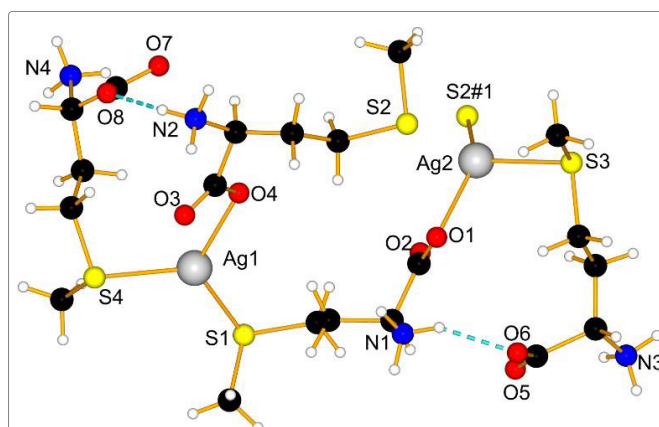


**Figure 6.** Crystal structure of {[Ag<sub>2</sub>(L-Met)<sub>4</sub>](NO<sub>3</sub>)<sub>2</sub>·2H<sub>2</sub>O}<sub>n</sub>. NO<sub>3</sub>- and H<sub>2</sub>O molecules have been removed to make it easier to understand. H-bonds are represented in dashed lines (CIF file (CCDC 1547635) from ref29).

Ag<sup>+</sup> binding. Furthermore, it was demonstrated how Ag<sup>+</sup> stabilizes  $\alpha$ -helical conformations in peptide models, in agreement with CD experiments<sup>31,33</sup>. Together, these results provide an initial step for predicting metal-binding behavior and conformational changes in proteins<sup>29,31-33</sup>. It is important to note that tetrapeptides offer a simplified model and that further studies on longer sequences and full-length proteins are necessary to fully understand metal-binding behavior.

More recently, Monneau *et al.* refined the structural and functional understanding of SilE using a combination of analytical and biophysical techniques (NMR, CD, SAXS, HRMS, CE-ICP-MS, IM-MS, and AlphaFold prediction)<sup>34</sup>. Their study confirmed that SilE contains up to eight potential binding sites, with four high-affinity sites. Ag<sup>+</sup> binding has been shown to induce the formation of four  $\alpha$ -helical segments, while the protein itself remains flexible, sampling elongated to more compact conformations.<sup>34</sup> The solvent-accessibility surface area of histidine and methionine residues is significantly increased in elongated forms, thereby facilitating efficient Ag<sup>+</sup> binding<sup>34</sup>. This dynamic structural organization enables SilE to function as a periplasmic metallochaperone, sequestering multiple Ag<sup>+</sup> and potentially delivering them to the tripartite efflux system SilABC while maintaining periplasmic Ag<sup>+</sup> homeostasis<sup>34</sup>.

## Conclusions

In conclusion, this mini review underlines the structural and functional parallels between the Sil and Cus systems in Gram-negative bacteria. The regulatory modules (SilSR and CusSR) control gene expression in response to metal stress, while the tripartite pumps (SilABC and CusABC) and periplasmic chaperones (SilF and CusF) coordinate metal ion export. SilP functions as an inner membrane ATPase, delivering Ag<sup>+</sup> to the periplasmic proteins, while SilG is

hypothesized to provide auxiliary support in Ag<sup>+</sup> transport. SilE, investigated through tetrapeptide, computational, and full-length protein studies, has been shown to bind up to eight Ag<sup>+</sup> via histidine- and methionine-rich motifs and undergo dynamic  $\alpha$ -helical rearrangements. Collectively, these results contribute to a more comprehensive understanding of the mechanism of Ag<sup>+</sup> sequestration and extrusion, highlight the additional functionalities of the Sil system in comparison to Cus, and establish a framework for future studies on bacterial silver tolerance and potential antimicrobial applications. However, the variation in reported Ag<sup>+</sup> binding capacities also underlines the influence of experimental approaches and methodological limitations, which should be considered when comparing and integrating data across studies.

Based on studies of longer peptide sequences, we suggest that the diversity of Ag<sup>+</sup> binding affinities observed at the peptide levels applies to larger segments and contributes to the overall binding behavior of SilE. This hypothesis must be validated through experimental investigations in the context of the full-length protein.

### Author Contributions

All authors contributed to writing and reviewing the final version and approved its submission.

### Acknowledgements

The authors thank the University of Fribourg, Fribourg Center for Nanomaterials, Swiss National Science Foundation (Project 2000020\_172777 and 2000020\_204215) for their generous support.

### Conflict of Interest

There are no conflicts to declare

### References

1. S. Eckhardt, P. S. Brunetto, J. Gagnon, M. Priebe, B. Giese, and K. M. Fromm, *Chem. Rev.*, 2013, **113**, 4708.
2. Y. A. Krutyakova, and A. G. Khina, *Appl. Biochem. Microbiol.*, 2022, **58**, 419.
3. N. Law, S. Ansari, F. R. Livens, J. C. Renshaw, and J. R. Lloyd, *Appl. Environ. Microbiol.*, 2008, **74**, 7090.
4. S. I. Vasylevskyi, S. Kracht, P. Corcoso, K. M. Fromm, B. Giese, and M. Füeg, *Angew. Chem. Int. Ed.*, 2017, **56**, 5926.
5. V. Chabert, L. Babel, M. P. Füeg, M. Karamash, E. S. Madivoli, N. Herault, J. M. Dantas, C. A. Salgueiro, B. Giese, and K. M. Fromm, *Angew. Chem. Int. Ed.*, 2020, **59**, 12331.
6. L. J. V. Piddock, *Nat. Rev. Microbiol.*, 2006, **4**, 629.
7. P. J. F. Henderson, C. Maher, L. D. H. Elbourne, B. A. Eijkelkamp, I. T. Paulsen, and K. A. Hassan, *Chem. Rev.*, 2021, **121**, 5417.
8. D. H. Nies, *FEMS Microbiol. Rev.*, 2003, **27**, 313.
9. C. P. Randall, A. Gupta, N. Jackson, D. Busse, and A. J. O'Neill, *J. Antimicrob. Chemother.*, 2015, **70**, 1037.
10. A. Gupta, K. Matsui, J.-F. LO, and S. Silver, *Nat. Med.*, 1999, **5**, 183.
11. G. L. McHugh, R. C. Moellering, C. C. Hopkins, and M. N. Swartz, *Lancet*, 1975, **1**, 235.
12. S. Silver, *FEMS Microbiol. Rev.*, 2003, **27**, 341.
13. J. A. Delmar, C.-C. Su, and E. W. Yu, *Biometals*, 2013, **26**, 593.
14. S. Franke, G. Grass, and D. H. Nies, *Microbiol.*, 2001, **147**, 965.
15. S. Franke, G. Grass, C. Rensing, and D. H. Nies, *J. Bacteriol.*, 2003, **185**, 3804.
16. S. A. Gudipaty, A. S. Larsen, C. Rensing, and M. M. McEvoy, *FEMS Microbiol. Lett.*, 2012, **330**, 30.
17. O. McNeilly, R. Mann, M. Hamidian, and C. Gunawan, *Front. Microbiol.*, 2021, **12**, 652863.
18. UniProt BLAST. Cambridge (UK): UniProt Consortium; 2002 [09.03.2026]. Available from: <https://www.uniprot.org/blast>
19. S. A. Gudipaty, and M. M. McEvoy, *Biochim. Biophys. Acta*, 2014, **1844**, 1656.
20. G. P. Munson, D. L. Lam, F. W. Outten, and T. V O'halloran, *J. Bacteriol.*, 2000, **182**, 5864.
21. R. M. Lithgo, M. Hanževački, G. Harris, J. J. A. G. Kamps, E. Holden, T. M. Gianga, J. L. P. Benesch, C. M. Jäger, A. K. Croft, R. Hussain, J. L. Hobman, A. M. Orville, A. Quigley, S. B. Carr, and D. J. Scott, *J. Biol. Chem.*, 2023, **299**, 105331.
22. C. Arrault, Y. R. Monneau, M. Martin, F. X. Cantrelle, E. Boll, F. Chirot, C. Comby Zerbino, O. Walker, and M. Hologne, *J. Biol. Chem.*, 2023, **299**, 105004.
23. I. R. Loftin, N. J. Blackburn, and M. M. McEvoy, *J. Biol. Inorg. Chem.*, 2009, **14**, 905.
24. F. Long, C. C. Su, M. T. Zimmermann, S. E. Boyken, K. R. Rajashankar, R. L. Jernigan, and E. W. Yu, *Nature*, 2010, **467**, 484.
25. F. Long, C. C. Su, H. T. Lei, J. R. Bolla, S. V. Do, and E. W. Yu, *Phil. Trans. R. Soc. B*, 2012, **367**, 1047.
26. R. Kulathila, R. Kulathila, M. Indic, and B. van den Berg, *PLoS ONE*, 2011, **6**, e15610.
27. M. Palmgren, *J. Biol. Chem.*, 2023, **299**, 105352.
28. S. F. Alquethamy, M. Khorvash, V. G. Pederick, J. J. Whittall, J. C. Paton, I. T. Paulsen, K. A. Hassan, C. A. McDevitt, and B. A. Eijkelkamp, *Int. J. Mol. Sci.*, 2019, **20**, 575.
29. V. Chabert, M. Hologne, O. Sénèque, A. Crochet, O. Walker, and K. M. Fromm, *Chem. Commun.*, 2017, **53**, 6105.
30. K. R. Asiani, H. Williams, L. Bird, M. Jenner, M. S. Searle, J. L. Hobman, D. J. Scott, and P. Soultanas, *Mol. Microbiol.*, 2016, **101**, 731.
31. V. Chabert, M. Hologne, O. Sénèque, O. Walker, and K. M. Fromm, *Chem. Commun.*, 2018, **54**, 10419.
32. A. Bianchi, F. Marquet, L. Manciocchi, M. Spichy, and K. M. Fromm, *Chem. Commun.*, 2025, **61**, 5309.
33. L. Manciocchi, A. Bianchi, V. Mazan, M. Potapov, K. Fromm, and M. Spichy, *Biophysica*, 2025, **5**, 7.
34. Y. Monneau, C. Arrault, C. Duroux, M. Martin, F. Chirot, L. Mac Aleese, M. Girod, C. Comby-Zerbino, A. Hagège, O. Walker, and M. Hologne, *Phys. Chem. Chem. Phys.*, 2023, **25**, 3061.